

# Dynamic soil parameters determination by geophysical prospecting in Mexico City: implication for site effect modeling

D. Jongmans, D. Demanet, C. Horrent

*Laboratory of Engineering Geology and Geophysical Prospecting, Liege University, Bat.B19, 4000 Liege, Belgium*

M. Campillo

*Laboratoire de Géophysique Interne et Tectonophysique, Université J. Fourier, BP 53X, F38401 Grenoble, France*

&

F. J. Sanchez-Sesma

*Instituto de Ingenieria, Unam, Ciudad Universitaria, Coyoacan, 04510 Mexico D.F., Mexico*

(Received 5 February 1996; accepted 16 March 1996)

Seismic experiments were conducted in Mexico City in order to determine the dynamic characteristics of the soft clay layer present at the surface in the lake bed zone. *In-situ* measurements of  $V_p$ ,  $V_s$ ,  $Q_p$  and  $Q_s$  were performed in the Texcoco lake area.  $Q_s$  values ranging from 8 to 60 have been found from the surface down to 30 m depth, while  $V_s$  values are between 30 and 115 m/s for the same depths. These relatively low  $Q$  values support the idea that surface waves generated at the edges of the Mexico basin cannot propagate very far in the structure. During this study, the elastic characteristics of the surficial basalt layers outcropping in the hill zone have also been investigated. Very low  $P$ -wave velocity values (500–800 m/s) have been found in the basalt. In the hill zone where basalts are interbedded with soil, numerical modeling has shown that such low values can only be partially explained by the relation between wavelength and basalt thickness and that other mechanisms, like fracturation, must be involved. Copyright © 1996 Elsevier Science Limited.

## 1 INTRODUCTION

For microzonation purposes, Mexico City is usually divided in three geotechnical zones (Fig. 1): the lake zone with 10–100 m of soft clay overlying sands; the transition zone with sandy and silty alluvium; and the hill zone, composed of volcanic flows and tuffs at the surface.<sup>1</sup>

After the 1985 Michoacan earthquake which caused huge damage in Mexico City, it has clearly appeared that the main cause of the catastrophe was a very large amplification effect in the lake zone, related to the presence of the shallow soft clay layer. Using spectral ratios of strong motions records, Singh *et al.*<sup>2</sup> observed an amplification in the lake zone as high as 50 relative to the hill zone. Besides amplification effect, the motion in

the lake zone is also characterized by very long durations which are observed for both weak and strong motions. At first, it has been thought that this phenomenon could result from the response of the large scale Mexico City basin. Despite numerous efforts including one-dimensional and two-dimensional modeling (for a review, see Chavez-Garcia and Bard<sup>3</sup>), the duration in the lake-bed zone is still not satisfactorily explained. If significant surface waves are generated at the edges of the basin, they seem to attenuate very quickly inside the basin.<sup>4</sup> One of the main unknowns in these computations is the  $Q_s$  value in the clay layer, for which no *in-situ* measurement is available.

One possible explanation for this very long duration could lie in more complicated two-dimensional or three-dimensional effects, considering both large scale and

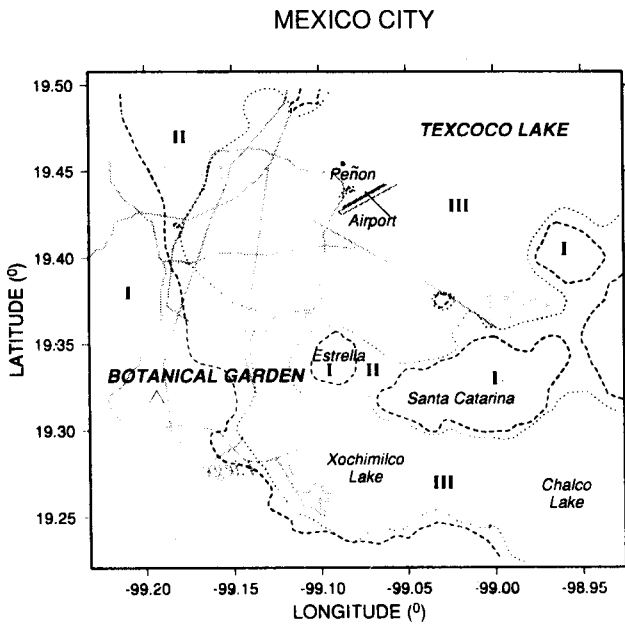


Fig. 1. Situation map with the geotechnical zones in Mexico City.

small scale effects. At the present day this combined effect is still difficult to simulate in an accurate way. Another explanation has recently been given by Singh and Ordaz<sup>5</sup> who proposed that the ground motions in the hill zone have already a long duration, at a lower amplitude than in the lake-bed zone.

Anyway, the dynamic characteristics,  $V_p$ ,  $V_s$ ,  $Q_s$  and  $Q_p$ , of the surficial clay layer have rarely been measured *in-situ* and it has appeared crucial to get reliable dynamic characteristic values as an input for the computations. When comparing motions in the lake-bed and in the hill zones, it is also important to know the dynamic properties of the basalt flow layers. That is why seismic experiments were performed in the lake zone and in the hill zone between March and May 1994.

Seismic prospecting was first conducted in the Texcoco lake, north-east to the Mexico City basin, which consists of clay sediments similar to those of the lake bed zone.<sup>1</sup> Secondly, sites in the botanical garden where basalt flows outcrop and overlie clay layers have also been investigated in Mexico City. Finally, some experiments were also conducted in a basalt quarry located south to Mexico City in the Chichinautzin range.

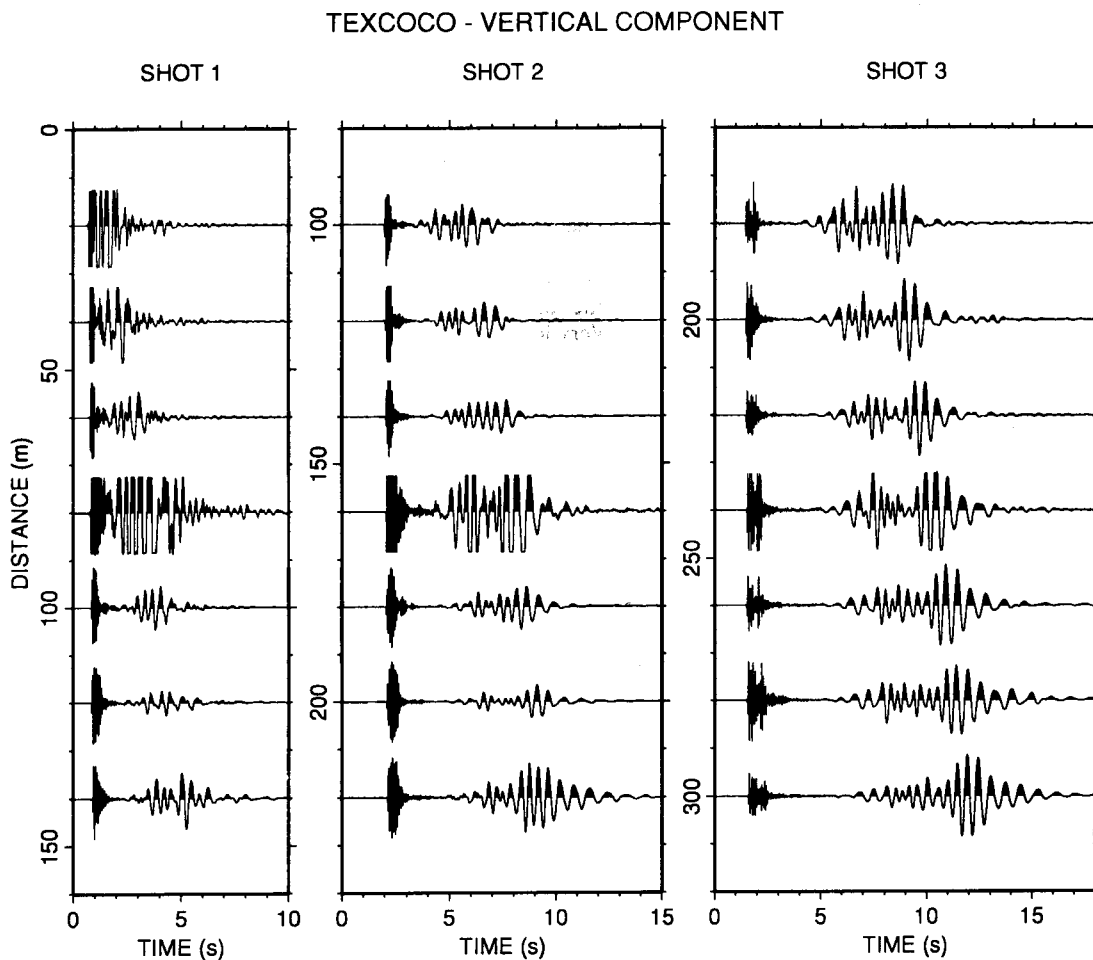


Fig. 2. Normalized seismograms (vertical component) recorded by accelerometers during three shots with different offsets (20, 100 and 180 m) in the Texcoco lake.

## 2 SEISMIC PROSPECTING AT THE TEXCOCO LAKE

### 2.1 Description of the experiment

The aim of the tests in the Texcoco lake was to determine the dynamic characteristics of the soft clay layer which plays an important role in the amplifications observed in the Mexico basin. Eight shots were performed in this area, five of which were recorded by 4.5 Hz vertical SENSOR geophones whereas the three other explosions were recorded by the same sensors and GURALD 3 components accelerometers. The offset between the source and the first geophone ranged from 5 to 180 m and the geophone spacing was between 2.5 and 20 m. The maximum profile length was then 320 m. The SENSOR geophones were connected to a PC-based acquisition system with 16 bits A/D converters and the GURALP accelerometers were attached to REFTEK stations. The relative times between the REFTEK stations were corrected with the arrival times measured on the PC-based acquisition which has a unique time base. Figure 2 presents the normalized signals (vertical component) recorded with accelerometers in the Texcoco lake for three shots fired at different offsets (shot 1: 20 m, shot 2: 100 m and shot 3: 180 m). The records exhibit very slow and high amplitude surface waves propagating at a velocity of about 30 m/s. Despite the relatively high dynamic range, *P*-waves, and more exceptionally *S*-waves, are slightly clipped on some records. Unfortunately, it was impossible for practical reasons to perform new experiments.

In addition to these eight *P*-wave profiles, a small profile (60 m long) was carried out for measuring *S*-wave velocities using the PC-based acquisition and 10 Hz horizontal geophones. For this refraction test, *SH* waves were generated by the horizontal impact of a hammer on the side of a loaded plank.

### 2.2 Wave velocity determination

The records have first been interpreted as refraction tests for the determination of the velocities  $V_p$  and  $V_s$ . For *P*-wave velocity determination, the data of all shots have been grouped together and the first arrivals were systematically picked on all the records. In our experiment the geophones stayed fixed and the source was moved. With this configuration, the hodochrones for the different shots only fit if the structure is horizontally layered. The agreement between arrival times, where an overlapping exists, is very good so the flat layer hypothesis does not seem too restrictive to obtain thickness and velocity values in the different layers. The interpretation was made with the method described by Mota.<sup>6</sup> The *P*-wave hodochrone (Fig. 3) yields a four-layer geometry at this site. The evolution of  $V_p$  values with depth is also shown in Fig. 3.

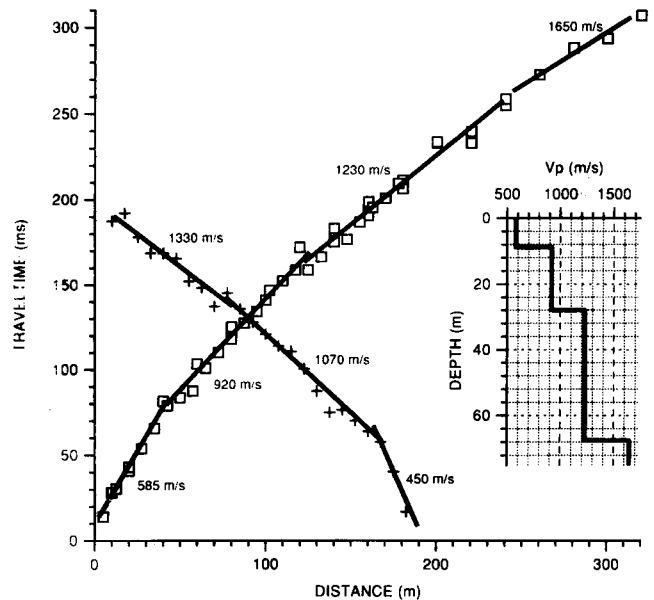


Fig. 3. *P*-wave hodochrones and velocity profile in the Texcoco lake.

As the *SH*-wave profile is 60 m long, only two layers are distinguished and the interpretation leads to very low *S*-wave velocities (30 and 60 m/s) in these two first layers. The thickness of the first layer is around 10 m.

*S*-wave velocity values have also been inferred by the surface wave inversion method which analyses the dispersion characteristics of the surface waves.<sup>7,8</sup> During classical refraction tests the recording time was increased in order to detect Rayleigh waves. Four data sets have been considered in this study, according to the shot and the receiver characteristics:

- set A 4.5 Hz geophones, shot 1;
- set B accelerometers, shot 2;
- set C accelerometers, shot 3;
- set D 4.5 Hz geophones, shot 3.

The Fourier spectra of the signals show that the energy band of the surface waves is mainly between 1 and 3 Hz. Thus, a significant part of the energy is removed by the 4.5 Hz geophone effect. The dispersion curves for phase velocity have been computed for each data set and two of them are illustrated in Fig. 4. Although some differences appear between the curves, they show a clear Rayleigh fundamental mode and are consistent in the prominent frequency range.

Phase velocity curves have been inverted for getting a *S*-wave velocity profile which is presented on Fig. 4 with the corresponding resolving kernels. The latter indicates that the resolution is relatively good down to about 25 m depth. The  $V_s$  model obtained from surface wave inversion is compared to the refraction results on Fig. 4. Both results show that the upper 10 m are characterized by very low  $V_s$  values (30 m/s). From 10 to 30 m (in the second layer shown by refraction tests),  $V_s$  values

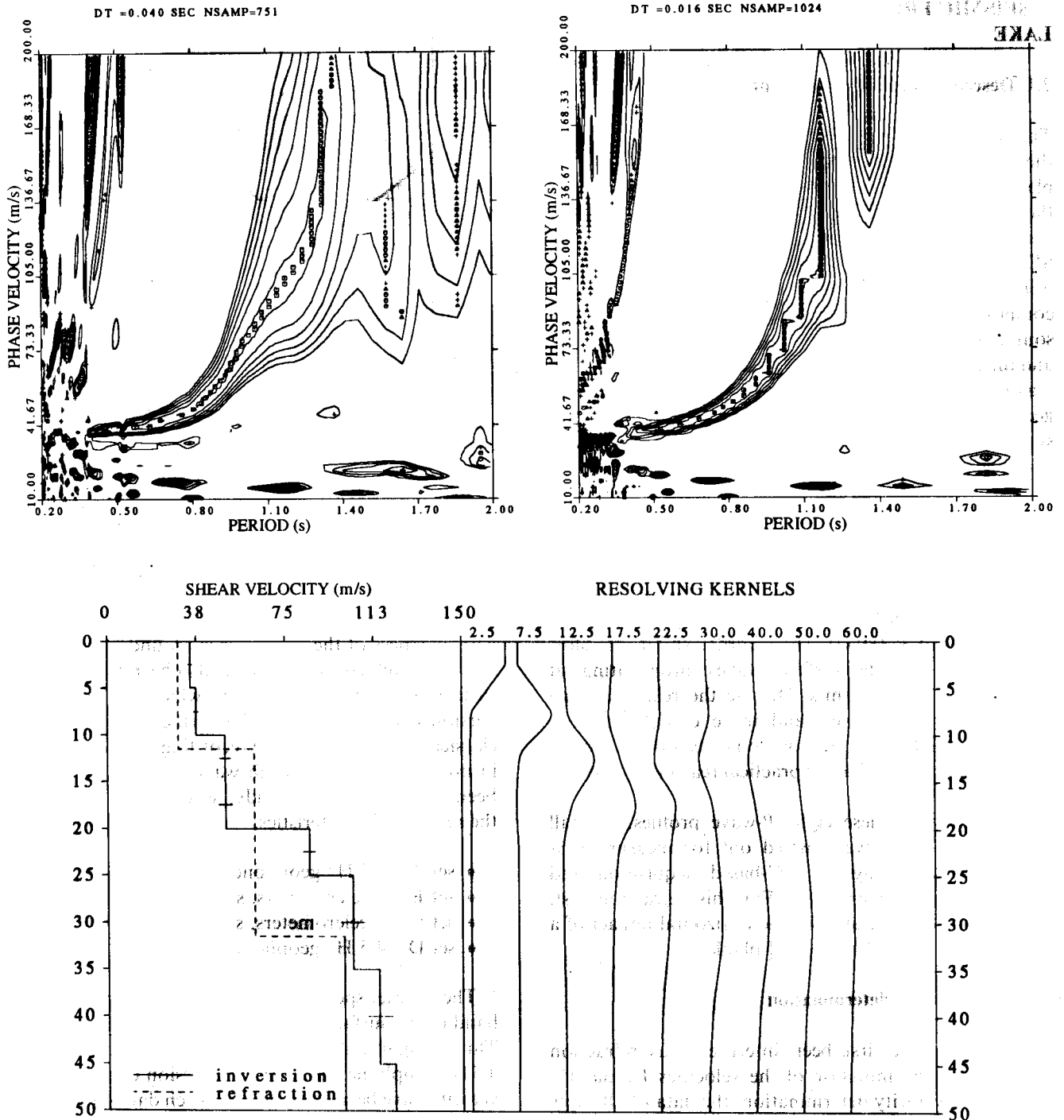


Fig. 4. Top: Phase velocity dispersion curves for shots 2 and 3 recorded by accelerometers and geophones, respectively; bottom:  $V_s$  profiles (surface wave inversion and refraction test) and resolving kernels.

increase from 50 to 100 m/s whereas, below 30 m depth,  $V_s$  is over 115 m/s.

### 2.3 Quality factor determination

$P$ -wave quality factor ( $Q_p$ ) values have been determined by two techniques: the rise-time and the spectral ratio methods while  $Q_s$  values have been inferred from the

surface wave attenuation. The rise-time method is based on the broadening of the pulse resulting from the attenuation of the high-frequency components. Gladwin and Stacey<sup>9</sup> defined the rise-time  $\tau$  as the ratio of the maximum peak amplitude to the maximum slope of the first quarter-cycle of the pulse. From their experiments, they proposed an empirical relationship based on the assumption that the broadening is proportional to the

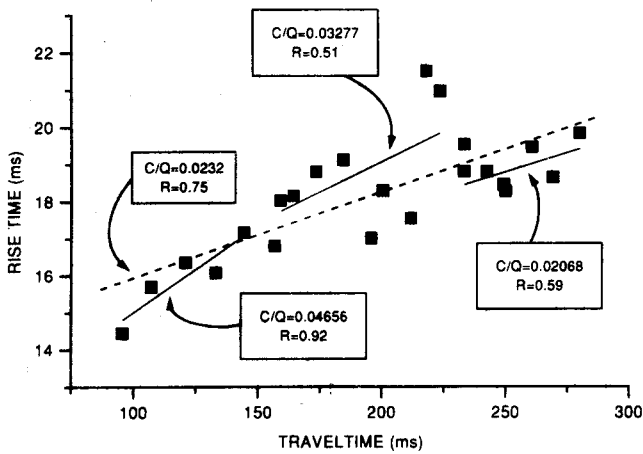


Fig. 5. Rise-time curve for data of shot 1. The dashed line represents the line fitting all the data while solid lines are for the three different layers.  $C/Q$  values are indicated with the correlation coefficient  $R$ .

traveltime:

$$\tau = \tau_0 + \frac{C}{Q} t \quad (1)$$

where  $\tau$  and  $\tau_0$  are the rise-time at the measurement point and at the source,  $t$  is the traveltime and  $C$  is a fixed constant. For velocity measures of an impulse source,  $C$  is theoretically equal to 0.3.<sup>10</sup> For realistic sources, Blair and Spathis<sup>11</sup> have however pointed out that  $C$  is source-dependent.

The rise-times have been measured for four shots recorded by 4.5 Hz phones. For these signals the frequency range is between 7 and 20 Hz. A typical graph of the rise-time vs the traveltime is shown on Fig. 5 for shot 1. The best line fitting the data has been determined for the different shots (dashed line on Fig. 5) and the slope

Table 1. Values of  $C$  and  $Q$  determined by the rise-time method (4.5 Hz geophones)

Layer	$C/Q$	$C$	$Q_p$
1 (550 m/s)	0.046	0.27	5.9
2 (920 m/s)	0.033	0.21	6.4
3 (1230 m/s)	0.0207	0.20	9.7

$C/Q$  has been computed. From other studies in soils,<sup>12</sup>  $C$  values usually range from 0.15 to 0.25. In this study,  $Q_p$  values calculated with  $C = 0.2$  are between 9 and 20.

Two improvements can however be made to  $Q$  determinations. The first is to consider the rise-time values in a same geological layer. This has been done for the data of Fig. 5 where three different layers may be distinguished from refraction interpretation. On this figure, the best fitting line for each layer are drawn with solid lines.

The second improvement consists in determining  $C$  values for each source. With this aim, several researchers<sup>11,13</sup> have proposed to simulate the wave propagation in an attenuating medium and to compare the results to the data. This method does not involve any assumption for the value of  $C$ . Since the pulse broadening is independent of the geometrical decay, plane waves are considered for the propagation.

Such procedure has been applied to the records of shot 1, for which the rise-time data show a separation between the different layers. The results are shown in Table 1. The obtained  $C$  values are between 0.2 and 0.27 and they lead to  $Q_p$  values ranging from 6 to 10.

The spectral ratio method is based on the exponential decay of spectral wave amplitude with frequency. From a pair of seismograms, the method consists of computing the Fourier transform of the two signals. It can be shown that the logarithm of the ratio of the Fourier spectra of

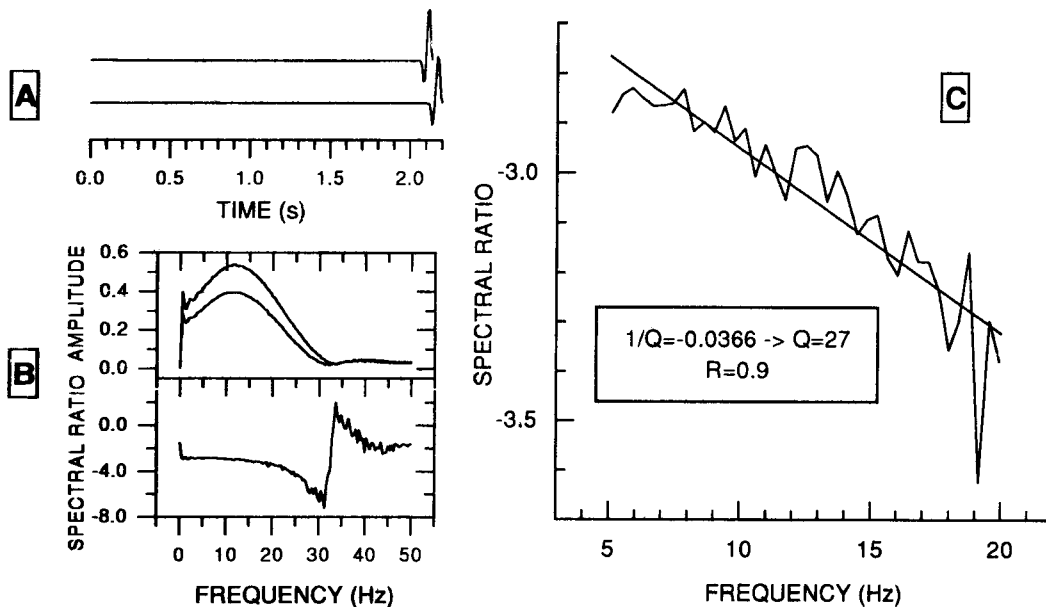


Fig. 6. A: Windowed  $P$ -waves for spectral ratio computations; B: Fourier spectra of the two signals and spectral ratio; C: spectral ratio on a limited frequency range and  $Q$  computation from the line slope.  $R$  is the correlation coefficient.

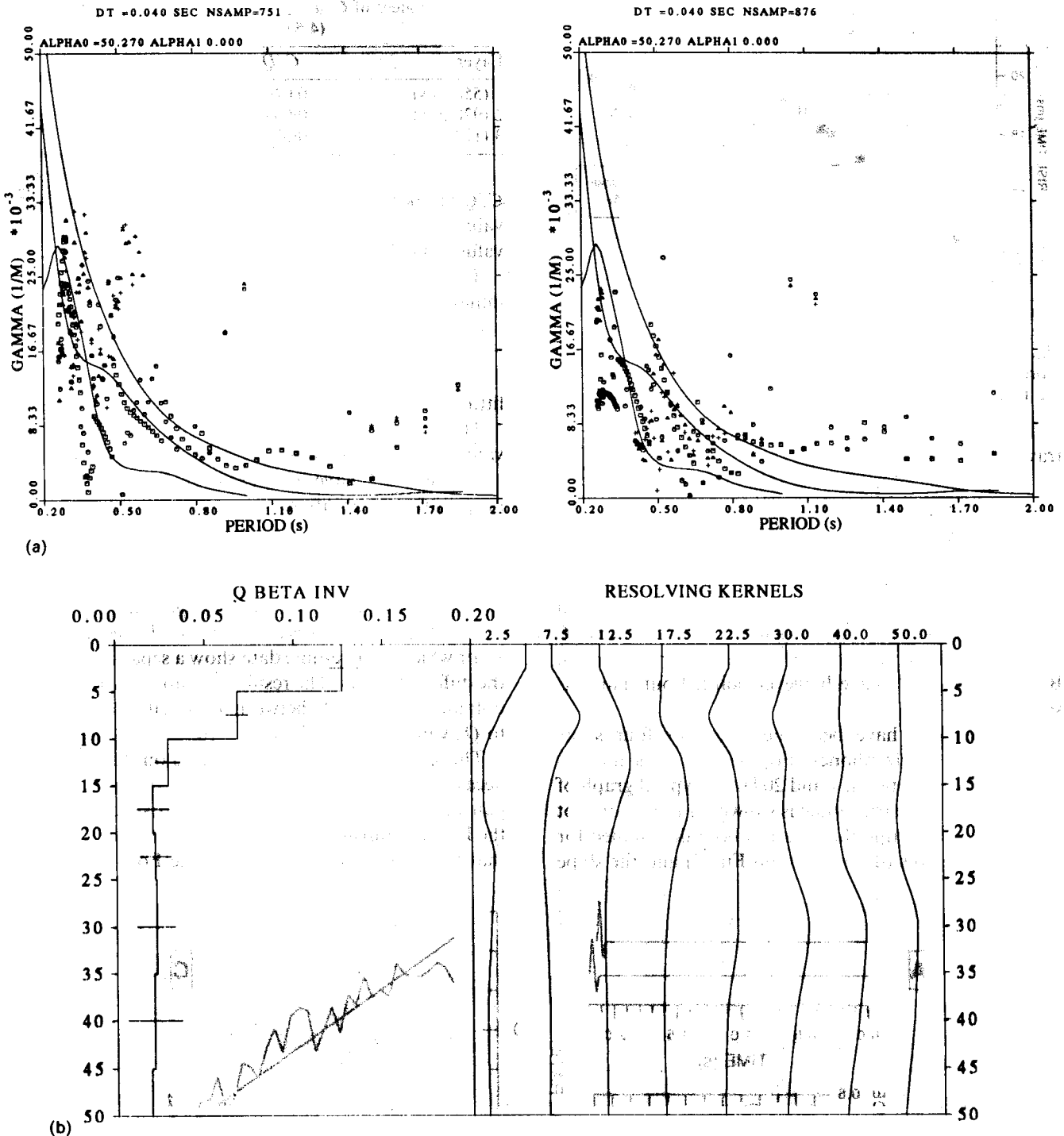


Fig. 7. A: Experimental surface wave attenuation dots for shots 2 and 3 with the three first theoretical modes (solid lines); B:  $Q_s$  vs depth profile and resolving kernels.

two signals decreases linearly with frequency and that  $Q$  values can be determined from the slope of the line. The spectral ratio method however suffers a few limitations: attenuation measurements have to be performed at a distance higher than one wavelength and the distance between the two sensors must be important enough to see the effect of the attenuation.<sup>12</sup> Another requirement is

Table 2.  $Q_p$  values determined by the spectral ratio method (Texcoco lake)

Layer	$V_p$ (m/s)	Distance of both geophones (m)	$Q_p$	Correlation coefficient $R$
3	1230	180–220	27	0.90
4	1650	260–300	32	0.74

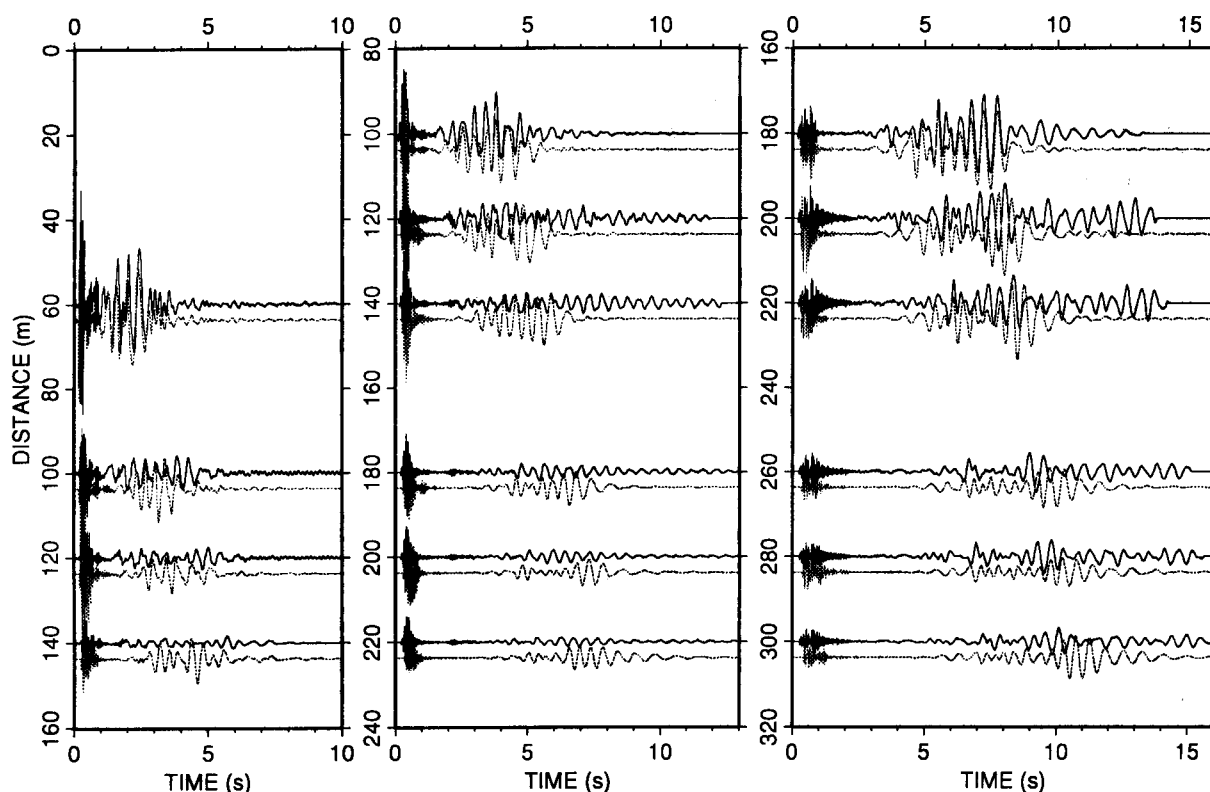


Fig. 8. Comparison between the recorded motions (dashed lines) and synthetic seismograms (solid lines) for the three shots measured by accelerometers.

to isolate a wave-train free from interference and then to window the very first arrival in the signal.

As only two signals are needed, accelerometer data have been used in this analysis. Due to the theoretical limitations mentioned above and to the signal to noise ratio, only four pairs of accelerograms have been selected. Two of them lead to a nonlinear diagram, suggesting that the pulses are not interference free. At least, two data sets may be used for spectral ratio analysis: one for layer 3 (1230 m/s) and one for layer 4 (1650 m/s). Figure 6 displays the windowed signals for shot 1, their Fourier spectra and the spectral ratio both for the whole frequency range and for the part where there is sufficient energy. Usually the frequency range is between 5 and 20 Hz. The linear regression slope gives the inverse of  $Q$  (Fig. 6). The results are given in Table 2. In the two cases, the spectral ratio method yields  $Q_p$  values around 30.

For  $Q_s$  determination, the attenuation of the surface waves has been studied using the program developed by Herrmann.<sup>7</sup> The attenuation coefficient  $\gamma$  vs period is

shown in Fig. 7. These diagrams are more scattered than the dispersion curves and an overlapping of different modes is very clear on some graphs.  $Q_s$  values deduced from inversion are given in Fig. 7.

In order to test the determined  $Q_s$  values, the theoretical attenuation curves of the first three modes have been calculated from this model and are superimposed on the observations in Fig. 7. The overlapping of the three modes allows us to explain the main features of the experimental data.

## 2.4 Conclusions

The main results obtained for the Texcoco lake are summarized in Table 3. These values are consistent with those found in the literature about Mexico City:  $V_s$  is very low (30–160 m/s) whereas  $V_p$  is more common (450–1650 m/s) for clay layers.  $Q_p$  and  $Q_s$  values increase with depth and range from 6 to 32 and from 8 to 60, respectively.  $Q_s$  values are higher than  $Q_p$  values, but

Table 3. Summary of the results of the seismic prospecting in the Texcoco lake.  $Q$  values were determined using the following methods: (rt) rise-time, (sr) spectral ratio, (sw) surface wave

Layer	Thickness (m)	$V_p$ (m/s)	$V_s$ (m/s)	$Q_p$ (from refraction tests)	$Q_s$ (from surface waves inversion)
1	8.8–11.5	450–550	30–38	6 (rt)	8–15 (sw)
2	20	920–1070	50–100	6 (rt)	34–48 (sw)
3	40	1230–1330	115–160	27 (sr)–10 (rt)	45–60 (sw)
4	—	1650	—	32 (sr)	—

**Table 4. Model used for the calculation of synthetic seismograms**

Layer	Thickness (m)	$V_p$ (m/s)	$V_s$ (m/s)	$Q_p$	$Q_s$
1	10	500	35	6	15
2	20	1000	80	6	30
3	40	1300	135	10	50
4	—	1650	135	30	50

they have been determined by different methods (rise-time and spectral ratios or surface wave inversion).  $Q_p$  values have been determined in the frequency range 5 to 20 Hz while  $Q_s$  are measured at lower frequency (1–3 Hz).

Our  $Q_s$  values are consistent with the results of Yang *et al.*<sup>14</sup> who found  $Q_s = 25$  in the clay at the SCT site, by applying the random decrement technique to acceleration records taken during the 19 September 1985 Mexico City earthquake. It must however be stressed out that these two *in-situ* measurements are taken at two different strain levels.

In order to test the determined velocity and quality factor values some numerical simulations of the shots in the Texcoco lake have been carried out, using the discrete wave number method developed by Bouchon.<sup>15</sup> Figure 8 shows the comparison for three shots between experimental signals and theoretical seismograms computed from the model of Table 4. Generally, synthetic seismograms exhibit a similar or lower amplitude than the real ones. This suggests that the determined  $Q$  values must be seen as a lower limit for numerical purposes.

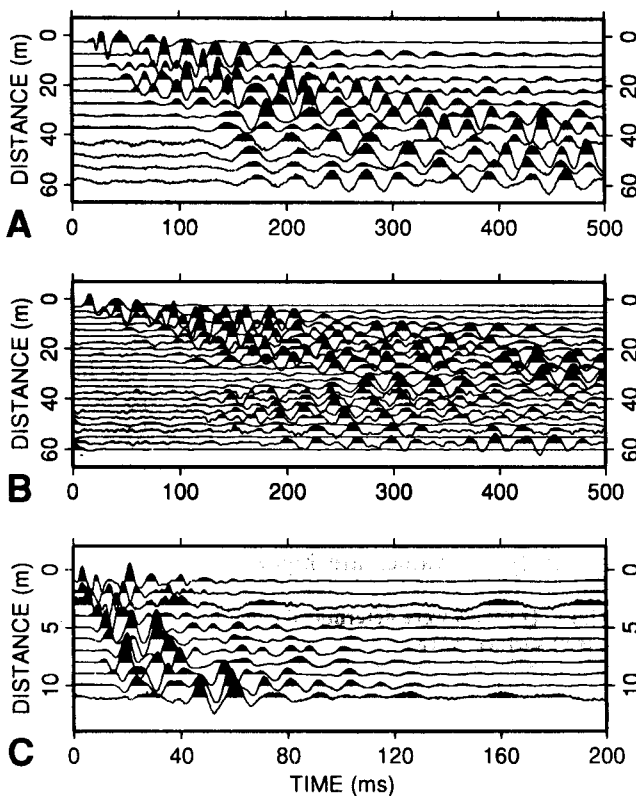


**Fig. 9.** Seismograms recorded during refraction tests in the botanical garden (A and B) and at the Parres quarry (C).

**Table 5. Laboratory tests on samples of basalt**

Length (mm)	Traveltime ( $\mu$ s)	Velocity (m/s)	Mass (g)	Specific mass ( $\text{g/cm}^3$ )
1 58.3	19.8	2944	128.4	1.89
2 44.7	14.5	3083	124.9	2.40
3 84.3	30.2	2791	202.0	2.06
4 96.4	37.1	2598	262.0	2.34

### 3 SEISMIC MEASUREMENTS IN BASALT ROCKS

#### 3.1 *In-situ* measurements

In the hill zone, soil layers are interbedded with basalt flows and some seismic tests were performed on basalt outcrops in order to determine its velocity. Two different sites have been investigated: the botanical garden (Fig. 1) located in the hill zone and the Parres basalt quarry (40 km south to Mexico City) in the Chichinautzin volcanic range.

Several seismic profiles have been carried out at different sites in the botanical garden of Mexico City, with a sledgehammer striking a steel plate as a source. Though the basalt outcrops are here and there in the garden, the signal to noise ratio was usually bad, preventing an accurate picking of the first phase. Figures 9A and B presents seismograms recorded at two sites in the botanical garden with two different layouts. At the second site (Fig. 9B), the geophones were set up directly on the outcropping rock. The signals have been bandpassed between 30 and 200 Hz to remove most of the noise. Interpretation of the two refraction tests leads to  $P$ -wave velocity values ranging from 460 and 600 m/s in the basalt surficial layer. Such surprising low  $V_p$  values have already been measured in this area by Benhumea Leon and Vazquez Contreras<sup>16</sup> during a large refraction campaign in the center of Mexico City. Records of quarry blasts along an east–west line in the same area (Singh, personal communication) has led to  $V_p = 1000$  m/s and  $V_s = 350$  m/s in the first 90 m consisting of a succession of basalt flows and interbedded soil layers.

A supplementary test was also carried out in the basalt quarry of Parres outside of Mexico City, where a lower noise level was expected. The signal to noise ratio is somewhat better, but still not very good (Fig. 9C). The outcropping basalt is characterized by a  $P$ -wave velocity as low as 440 m/s down to 10 m. Below this layer  $V_p$

**Table 6. Dynamic characteristics used for the modeling**

Model	Layer	Thickness (m)	$V_p$ (m/s)	$V_s$ (m/s)	$Q_p$	$Q_s$
1	basalt	15	2500	1500	100	100
	clay		1300	130	20	20
2	basalt	15	2500	600	100	100
	clay		1300	130	20	20
3	shallow 1.	2	500	150	20	20
	basalt	13	2500	600	100	100
	clay		1300	130	20	20



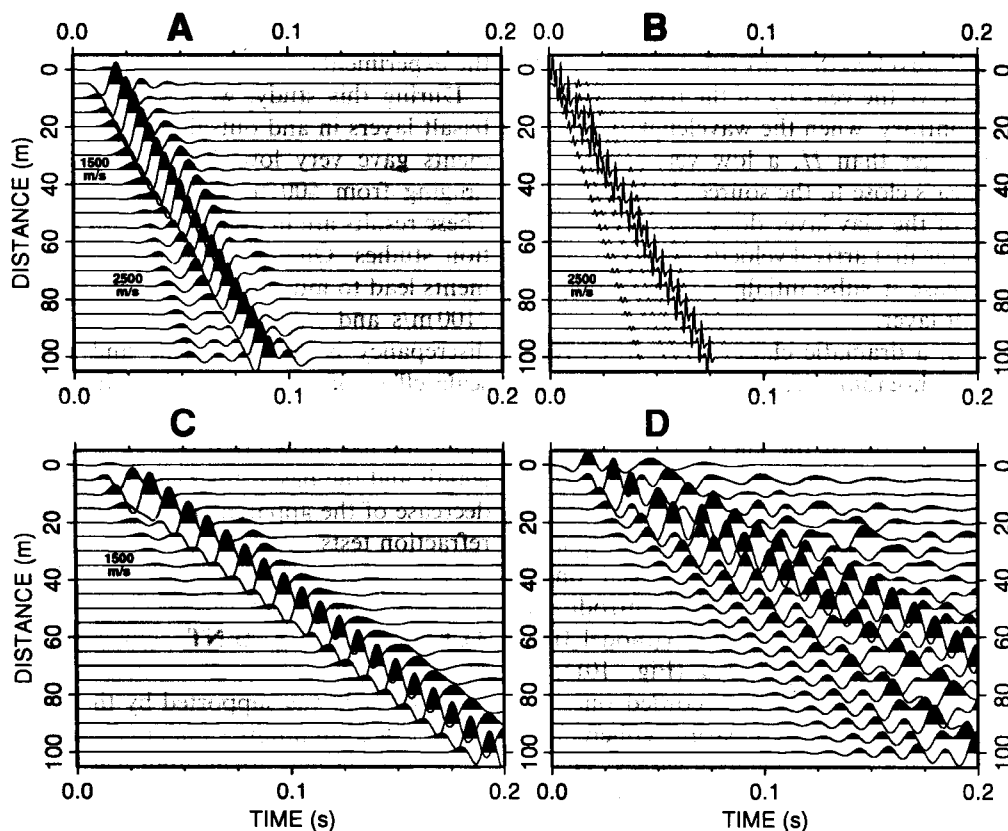


Fig. 10. Synthetic seismograms computed for the models of Table 6 with a Ricker wavelength of frequency  $fR$  as a source; A: model 1 and  $fR = 50$  Hz; B: model 1 and  $fR = 500$  Hz; C: model 2 and  $fR = 50$  Hz; D: model 3 and  $fR = 50$  Hz.

values are around 770 m/s. These results corroborate the values obtained in Mexico City.

### 3.2 Laboratory tests

Laboratory measurements of the  $P$ -wave seismic velocity have been made on four samples taken on outcrops of basalt in the botanical garden and in Parres. The results are given in Table 5.

With a specific mass of the samples varying between 1.89 and 2.40,  $P$ -wave velocity values are ranging from 2600 to 3100 m/s. Additional tests on the same samples have been performed in a triaxial cell to get  $V_s$  values. Under a pressure of 2 kPa, the following results were obtained:  $V_s = 1790$  m/s ( $\pm 360$  m/s) and  $V_p = 3930$  m/s ( $\pm 120$  m/s).

The differences between the velocity values obtained from *in-situ* tests ( $V_p = 440$ – $800$  m/s) and laboratory measurements ( $V_p = 2600$ – $3100$  m/s) are very high. This apparent discrepancy could result from two phenomena:

(1) A scale effect; the *in-situ* measurements take into account the fracturation in the rock mass, especially polygonal fractures resulting from cooling, whose effect is not considered during laboratory tests at the scale of the sample ( $\pm 5$  cm).

(2) An influence of the wavelength on the velocity values. Laboratory tests typically use frequencies around

a few hundreds kHz while the frequency range during field studies is between 10 and 100 Hz. This difference of wavelength may have an influence when a relatively thin layer of basalt overlies a soft soil layer, which is a typical configuration in the hill zone. In the botanical garden, the basalt thickness may be evaluated to 10–15 m (from investigations during the subway excavation), which is much lower than the seismic wavelength. In this case, the apparent  $P$ -wave velocity may be very different from the basalt velocity. This hypothesis will be evaluated by numerical modeling.

## 4 MODELING OF THE RESPONSE OF A BASALT LAYER OVERLYING SOFT SOIL

Some numerical simulations were performed in order to evaluate the apparent  $P$ -wave velocity measured on a basalt layer overlying clay deposits. The dynamic characteristics of the two materials are given in Table 6 for three different configurations. In these models,  $P$ -wave velocities in the basalt and the clay have been fixed to 2500 and 1300 m/s, respectively, and the  $V_s$  value in the clay to 130 m/s.

Synthetic seismograms were computed using the discrete wavenumber method and a Ricker wavelet as a source. First, the relation between the seismic wavelength and the basalt thickness  $H$  has been studied for

model 1 (Fig. 10A and B). At high frequency ( $fR = 500$  Hz), the  $P$  wavelength (5 m) is lower than  $H$  and the first arrivals have the velocity of the basalt layer (2500 m/s). On the contrary, when the wavelength (50 m for  $fR = 50$  Hz) is larger than  $H$ , a low velocity first wave (1500 m/s) appears close to the source. Decreasing the  $P$ -wave velocity of the clay layer does not lead to a significant change of the first arrival velocity and we have been unable to decrease it substantially when keeping 2500 m/s in the basalt layer.

On the other hand, a dramatic change (Fig. 10C) is observed on the seismograms if the basalt  $S$ -wave velocity becomes lower than the clay  $P$ -wave velocity (model 2). In this case, most of the energy propagates through low velocity surface waves and the 1500 m/s fastest wave strongly attenuates with distance. In the presence of noise, surface waves can be picked as the first arrivals, but no such coherent phases are seen on experimental seismograms (Fig. 9). However, introducing a shallow weathered layer at the basalt top (model 3) leads to more complicated seismograms (Fig. 10D) with signal shapes more similar to the recorded ones. In this case it appears difficult to measure coherent arrival times giving correct  $P$ -wave velocity values. The assumption that the basalt  $S$ -wave velocity is low does not, however, seem to be supported by laboratory measurements, but one cross-hole test,<sup>16</sup> carried out inside the university site, has led to  $V_s$  values lower than 300 m/s in the basaltic upper layer (4 m thick) outcropping in this area.

Therefore, the influence of a wave frequency effect on the  $P$ -wave velocities can only partially explain the observed low values and another mechanism, such as fracturation, must be involved.

## 5 CONCLUSIONS

Seismic prospecting experiments were performed in Mexico City in order to determine the dynamic characteristics of the clay layer, which lies over the lake bed zone and of the basalt flow layers, which outcrop in the hill zone.

For clay property determinations, seismic tests were conducted in the Texcoco lake. The results show very low  $V_s$  values ranging from 30 m/s at the surface to 115 m/s at 40 m depth while  $V_p$  values increase from 500 to 1650 m/s for the same depths.  $Q_p$  and  $Q_s$  values increase with depth and range from 6 to 32 and from 8 to 60, respectively. These relatively low values show that surface waves generated at the edges of the Mexico basin can not propagate very far within the lake bed zone. It must be stressed however, that our  $Q$  determinations are made in a higher frequency range (1–20 Hz) than the dominant frequency (0.5 Hz) used in the computations. The parameter values have been

checked by simulating the wave propagation during the experiments.

During this study, we also investigated the surficial basalt layers in and outside Mexico City. *In-situ* experiments gave very low  $P$ -wave velocities, more or less ranging from 500 to 800 m/s in the first 15 m depth. These results are in agreement with two previous refraction studies. On the other hand, laboratory measurements lead to much higher values ( $V_p$  between 2600 and 3100 m/s and  $V_s$  around 1790 m/s). The origin of this discrepancy is still not clear and may result from a scale effect of the fracturation. In the hill zone where basalt layers are interbedded with soils, numerical modeling has shown that the relation between the wavelength and the basalt thickness could partially explain a decrease of the apparent  $P$ -wave velocity determined by refraction tests.

## ACKNOWLEDGEMENT

This research was supported by the Commission of the European Communities under contract no. CI1\*-CT92-0036. The seismic prospecting was performed with the help of J. L. Rodriguez Zuniga, J. Ramos Martinez and E. Romero Jimenez. We thank J. F. Couvreur from the Unité du Génie Civil, Catholic University of Louvain and C. Schroeder from LGIH, Liege University, for performing the laboratory tests.

## REFERENCES

1. Romo, M. P., Jaime, A. & Resendiz, D. The Mexico earthquake of September 19, 1985—general soil conditions and clay properties in the valley of Mexico. *Earthq. Spectra*, 1988, 4, 731–752.
2. Singh, S. K., Lermo, J., Dominguez, T., Ordaz, M., Espinosa, J. M., Mena, E. & Quaas, R. A study of amplification of seismic waves in the valley of Mexico with respect to a hill zone site (CU). *Earthq. Spectra*, 4, 653–673.
3. Chavez-Garcia, F. J. & Bard, P. Y. Site effects in Mexico City eight years after the September 1985 Michoacan earthquakes. *Soil Dyn. Earthq. Engng*, 1994, 13, 229–247.
4. Bard, P. Y., Campillo, M., Chavez-Garcia, F. J. & Sanchez-Sesma, F. The Mexico earthquake of September 19, 1985—a theoretical investigation of large- and small-scale amplification effects in the Mexico City valley. *Earthq. Spectra*, 1988, 4, 609–633.
5. Singh, S. K. & Ordaz, M. On the origin of long coda observed in the lake bed strong-motion records of Mexico City. *Bull. Seismol. Soc. Am.*, 1993, 83, 1298–1306.
6. Mota, L. Determination of dips and depths of geological layers by the seismic refraction method. *Geophys.*, 1964, 19, 242–254.
7. Herrmann, R. *Computer Programs in Seismology*. Vol. 6, St Louis University, MO.
8. Jongmans, D. L'influence des structures géologiques sur l'amplification des ondes sismiques. Mesures in-situ et modélisation. *Coll. des publ. de la Fac. des Sc. Appl.* no. 131.

9. Gladwin, M. T. & Stacey, F. D. Anelastic degradation of acoustic pulses in rock. *Phys. Earth Planet. Int.*, 1974, **8**, 332–336.
10. Kjartansson, E. Constant  $Q$ -wave propagation and attenuation. *J. Geophys. Res.*, 1979, **84**, 4737–4748.
11. Blair, D. P. & Spathis, A. T. Seismic source influence in pulse attenuation studies. *J. Geophys. Res.*, 1984, **89**, 9253–9258.
12. Jongmans, D. *In situ* attenuation measurements in soils. *Engng Geol.*, 1990, **29**, 99–118.
13. Campillo, M. Sismogrammes synthétiques dans les milieux élastiques hétérogènes, PhD thesis, Grenoble University, pp. 221, 1986.
14. Yang, J. C. S., Qi, G. Z., Pavlin, V. & Durelli, A. J. *In-situ* determination of soil damping in the lake deposit area of Mexico City. *Soil Dyn. Earthq. Engng*, 1989, **8**, 43–52.
15. Bouchon, M. A simple method to calculate Green's functions for elastic-layered media. *Bull. Seism. Soc. Am.*, 1981, **71**, 959–971.
16. Benhumea Lon, M. & Vazquez Contreras, A. Estudios geofísicos del valle de Mexico, Comision Federal de Electricidad, Subdireccion de Construccion, Mexico, D.F., 1988.